Angewandte Chemie International Edition

DOI: 10.1002/anie.201305812

Ammonia Synthesis

The Haber–Bosch Process Revisited: On the Real Structure and Stability of “Ammonia Iron” under Working Conditions**

Timur Kandemir, Manfred E. Schuster, Anatoliy Senyshyn, Malte Behrens, and Robert Schlögl**

Dedicated to the Ammonia Laboratory of BASF SE in Ludwigshafen on the occasion of the 100th anniversary of the Haber–Bosch process

Ammonia synthesis is among the most important processes in the chemical industry. It was developed at BASF one hundred years ago based on the fundamental work of Fritz Haber[1] and process engineering by Carl Bosch. Haber combined feed gas recycling with the application of high pressure and an effective catalyst, for example, osmium, to achieve sufficiently high conversions of nitrogen according to the reaction $N_2 + 3H_2 \rightarrow 2NH_3$. This success led to the large-scale production of artificial fertilizers and today, approximately 80% of the worldwide ammonia output of 136 megatons[2] (2011) is used for this purpose.

Only little has changed in the actual ammonia synthesis step.[3] It is conducted at typical temperatures of 500 °C and pressures around 200 bar, resulting in ammonia concentrations in the exhaust gas of up to 18 vol%. A key development in the modern Haber–Bosch process was the unique catalyst synthesis developed at BASF by Alwin Mittasch in the early 20th century.[4] To achieve a highly active iron catalyst, magnetite (Fe_3O_4) was promoted by fusing it with irreducible oxides (K_2O, Al_2O_3, later also CaO) in an oxide melt. The fused magnetite is mechanically granulated and carefully reduced in the syngas feed to finally give the α-Fe catalyst.[5] This special synthesis leads to certain crucial properties of the resulting α-Fe phase, which is commonly termed “ammonia iron” and still used in industry today.

Ammonia synthesis has always been a test case for the maturity of catalysis science opposed to an already mature technology for the understanding of heterogeneous catalysis and for the scientific maturity of this research area. Today, due to tremendous efforts in surface science, physical and theoretical chemistry, and chemical engineering, a consistent picture of the reaction mechanism and of the role of the Fe catalyst and its promoters has emerged. Key contributions to the modern understanding of the ammonia synthesis reactions were elaborated by the research groups led by Gerhard Ertl,[6] Michel Boudart,[7] Gabor Somorjai,[8] Haldor Topsøe,[9] and Jens K. Nørskov,[10] just to mention a few. However, even after 100 years of application and research there still is scientific interest in the Haber–Bosch process as a gap remains between the fundamental experiments and the actual industrial process. Model studies conducted with well-defined, simplified materials with clean surfaces at low pressures contribute to the current knowledge of ammonia synthesis. The resulting so-called pressure and materials gaps prevent straightforward extrapolation of these results to the industrial process. Thus, the question of a dynamic change of the catalyst under actual reaction conditions remains to be studied by in situ experimentation.

It is well known from steel hardening[11] and catalytic ammonia decomposition[12] that iron can be easily nitrided by ammonia. The dissociative chemisorption of dinitrogen on the iron surface is the rate-limiting step in ammonia synthesis[6a] and opens possibilities for the subsurface diffusion of atomic nitrogen.[8] Ertl et al. proposed that the surface dissolution of nitrogen into iron forms a surface nitride of the approximate composition Fe_2N and that metastable γ-Fe_4N is formed in situ,[6a] while Herzog et al. proposed the formation of subnitrides of the type $Fe_{10-20}N$ based on a diffraction study on an industrial material, but at ambient pressure.[13] The partial pressures of ammonia and hydrogen determine the thermodynamic nitriding ability of the gas stream and the formed phases.[11a] In the Haber–Bosch process, p_{NH_3} is high due to the high total pressure and the relatively high product concentration. According to the Lehrer diagram,[11a] the existence of metastable γ′-FeN (fcc Fe sublattice, ca. 20 atom% N) or ε-FeN (hcp, 15–33 atom% N) is thermodynamically expected at the partial pressures of the Haber–Bosch process (see the Supporting Information). The discrimination of these bulk iron nitrides from α-Fe (bcc, < 0.4 atom% N) by diffraction is straightforward, as they have different crystal structures.[11e] However, the (reversible) formation of these Fe-N phases in the ammonia synthesis has not been observed directly so far, which might be explained by the lack of experimental methods suitable under these demanding conditions. Thus, the (in situ) nitriding of the ammonia synthesis catalysts has been the subject of debate.[13–15]

---

[*] T. Kandemir, Dr. M. E. Schuster, Dr. M. Behrens, Prof. Dr. R. Schlögl
Abteilung Anorganische Chemie
Fritz-Haber-Institut der Max-Planck-Gesellschaft
Faradayweg 4-6, 14195 Berlin (Germany)
E-mail: behrens@fhi-berlin.mpg.de
acsek@fhi-berlin.mpg.de

Dr. A. Senyshyn
Forschungsneutronenquelle Heinz Maier-Leibnitz (FRM II)
Technische Universität München
Lichtenbergstrasse 1, 85747 Garching (Germany)

[**] We thank F. Girgsdies for help with the phase analysis, M. Hölzl and S. Pfanzelt for support at the beamline, Friedrich K. Seitz and Frank Rosowski (BASF SE) for providing the catalyst and for fruitful discussions, and FRM II (Garching) for the allocation of beam time.

Supporting information for this article is available on the WWW under http://dx.doi.org/10.1002/anie.201305812.

Herein, we report in situ neutron diffraction studies of an industrial catalyst under conditions close to those of the Haber–Bosch process to determine whether dynamic bulk nitridation occurs. This method and the experimental setup were recently employed for the direct in situ observation of the bulk structural properties of working catalysts.[16] Ammonia synthesis was conducted on an industrial catalyst provided by BASF in a tubular fixed-bed reactor made of a nickel alloy at conditions of 425 °C and 75 bar determined by the safety limits of the setup. Syngas ($N_2/D_2 = 1{:}3$) was fed through the catalyst bed at a low space velocity to approach the thermodynamic equilibrium of the ammonia synthesis reaction, which corresponds to a product concentration of 14.7 vol % NH_3 (measured: 12.6 vol % ND_3). The experiment was performed at the SPODI beamline[17] of FRM II. The reactor walls and the catalyst bed were penetrated by the neutron beam during the experiment and high-resolution neutron diffraction data was recorded. According to the phase diagram, the conditions are sufficient for the formation of iron nitrides. At 425 °C and 75 bar the transition from the α-phase to the γ′-phase occurs at approximately 0.9 vol % NH_3 for pure iron, while the ε-phase is expected at 7.6 vol % NH_3. Milder conditions were applied before and after the reaction to check for reversible changes.

In Figure 1, the neutron diffraction pattern of the postreaction industrial catalyst is compared to those of two reference materials, commercial iron (α-Fe) and iron nitride ($Fe_{2-4}N$). The commercial iron nitride was prepared from iron by nitridation with ammonia and quenching. In the pattern of this reference sample, the γ′-Fe_4N_{1-y} (63 wt %), ε-$Fe_3N_{1.245}$ (24 wt %), and ε-Fe_3N_1 (13 wt %) phases of iron nitride can be identified. As seen from the comparison and confirmed by Rietveld refinement, all peaks of the Fe phase in the postreaction catalyst can be explained by the presence of α-Fe, and a phase transformation induced by nitridation leading to a stable bulk iron nitride can be excluded.

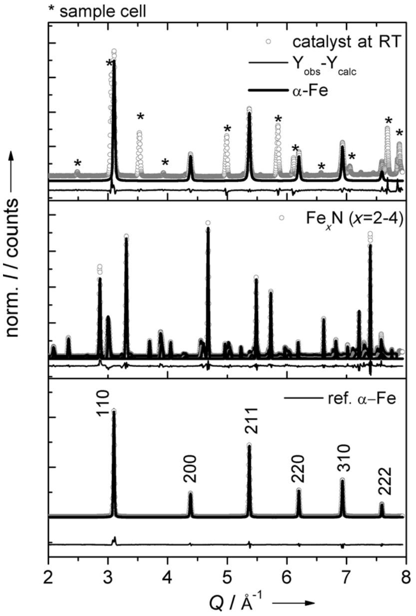

Figure 1. Neutron diffraction patterns and Rietveld refinements of commercial iron powder (bottom) and iron nitride (middle, $Fe_{2-4}N$) and the postreaction industrial ammonia synthesis catalyst at room temperature (top). Rietveld refinement revealed the presence of α-Fe (black profile) and peaks due to the reactor cell walls (marked). Y = Intensity.

To check for the possibility of the reversible formation of a metastable Fe-N phase during operation, as expected from the phase diagram, we compared the patterns of the activated catalyst in the prereaction state and of the fresh catalyst at 425 °C and 75 bar at time-on-stream (TOS) = 0 h, and the in situ pattern recorded at a self-generated NH_3 (viz. ND_3) concentration of 12.6 vol % at TOS = 88 h as well as of the postreaction state (Figure 2). In addition to the peaks of the metallic iron, a faint contribution of an additional magnetite phase (Fe_3O_4, see the Supporting Information) was observed in the prereaction catalyst. The presence of magnetite is a consequence of the kinetic difficulty to fully reduce the catalyst, and single-crystalline magnetite particles are proposed to act as spacers to prevent the metallic Fe platelets from sintering.[18] However, the crystalline magnetite disappeared at TOS = 26 h due to the high reducing potential of the syngas at working conditions and the catalyst is found to be in a strongly reduced state.[19] The lattice parameter of α-Fe is constant at 288.43 pm during ammonia synthesis at 425 °C.

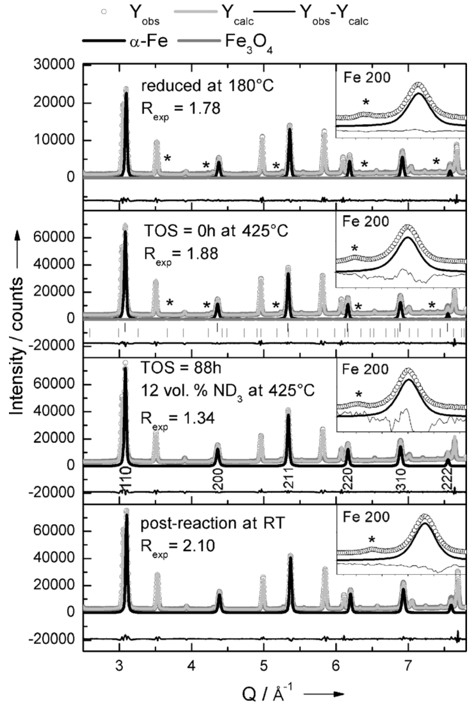

Figure 2. Neutron diffraction patterns of the ammonia synthesis catalyst under different conditions. The black line indicates the fitted contribution α-Fe phase to the patterns. a) Reduced, initial catalyst in 4.4 bar D_2 at 180 °C (the dark gray line is the profile of magnetite, peaks additionally marked by asterisks). b) Prereaction catalyst at 425 °C under 75 bar syngas at TOS = 0 h. c) In situ reaction state at 425 °C under 75 bar syngas, which is converted to yield 12 vol % ND_3 at TOS = 88 h. d) Postreaction catalyst in 75 bar Ar at room temperature. The insets show the magnification of the 200 peak of α-Fe, wherein the black asterisks marks the contribution from the Ni reactor tube.

After cooling, it is again similar that of the reference α-Fe at room temperature (286.79 pm versus 286.78 pm).

It is evident from Figure 2 that no in situ transformation into metastable bulk nitrides has taken place due to the inclusion of nitrogen atoms from the generated ammonia despite the high p_{NH_3} (viz. p_{ND_3}). Like the postreaction state (Figure 1), the catalyst under working conditions can be described to a first approximation by a single α-Fe phase. We can safely conclude that the virtual pressure of nitrogen during the experiment was not sufficient for nitriding of the bulk, because no peaks of the $Fe_{2-4}N$ reference pattern (Figure 1) were observed at any time. Such phases were recently described[11f] and are commonly observed in Fe-based catalysts for ammonia decomposition.

In comparison with the α-Fe reference, the peak profiles of the catalyst are significantly broadened (Figure 3), indicating a difference in the microstructure of the two materials. Also the intensity ratio of the α-Fe peaks differs for the reference anisotropic peak broadening of the 200 and 310 profiles; this might be related to the presence of endotactic chemical impurities in the lattice of the α-Fe host lattice (see the Supporting Information).[9,19,20] These observations clearly indicate that the preparation and activation process and/or additives have an effect on the microstructure and texture of the catalyst. Earlier studies revealed that the activated ammonia catalyst shows a strongly hierarchical microstructure[21] with Fe platelets in the near-surface region.[19] Therefore, the deviation of the catalyst's peak intensities and breadths from those of the α-Fe powder reference[22] can be interpreted as "structural anisotropy" of the ammonia iron caused by defects and size and strain effects.[23] It seems likely that the unexpected stability of the α-Fe phase in the catalyst is related to these microstructural effects.

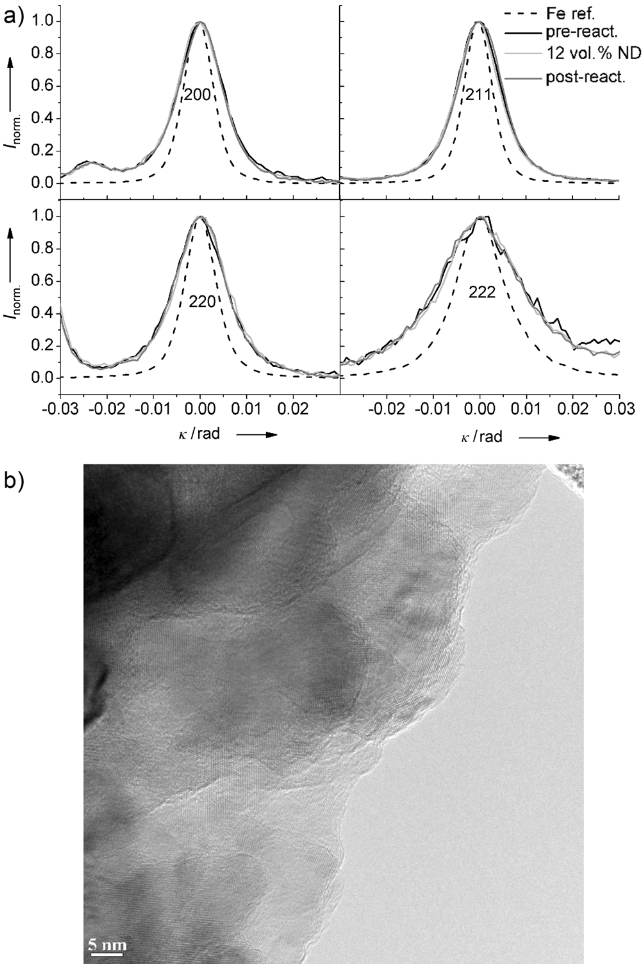

Figure 3. a) Normalized peaks profiles of the 200 (top left), 211 (top right), 220 (bottom left), and 222 (bottom right) of the catalyst's α-Fe reflections. The thermal shift [reference iron (dashed line), and post-reaction state (dark gray line): 28 °C; prereaction state (black line): 180 °C; in situ ammonia synthesis (light gray line): 425 °C] was compensated by normalizing to the peak maxima on the *x*-axis. b) Representative HRTEM image of the postreaction ammonia catalyst.

While the difference between catalyst and reference was apparent, it was surprising to see hardly any changes in the peak shapes of the catalyst when the conditions were changed (Figures 2 and 3). This observation strikingly confirms the stability not only of the iron bulk against nitridation, but also of the catalyst's unique microstructure. After the activation procedure, neither thermal annealing of defects, nor any major reversible or irreversible change of the catalyst's structural features could be clearly observed. The only faint variation of the peak breadths corresponds to a slight growth of the apparent domain size of α-Fe with the time-on-stream from (26 ± 5)nm (TOS = 0 h), which is in good agreement with earlier reports,[20b,24] to (32 ± 7) nm (TOS = 88 h). The structural stability of the α-Fe phase in the catalyst and of its lattice imperfections suggest that the crucial properties of "ammonia iron" have been developed already during the catalyst's activation in the feed gas and not during the actual ammonia synthesis experiment at higher p_{NH_3} (viz. p_{ND_3}).

We emphasize that the interpretation of the above results is largely consistent with and a confirmation of the established view of the active catalyst. The non-nitridated α-Fe clearly is the major phase of the catalyst, limiting possible nitrogen dissolution to a small fraction of the catalyst located at the surface of the large aggregates ($d \approx 100$ nm).[22] This results in a situation that can be described as a Fe-N surface phase (0.8–0.96 monolayers),[6d,25] which is not detectable by diffraction, and supported on a core of unaffected α-Fe, which dominates the diffraction pattern. This picture is in agreement with the model that the bulk α-Fe provides the support for a surface Fe species, which is supposed to play the crucial role in the catalytic process.[13,18,19,26] A representative high-resolution TEM image of the near-surface region of the postreaction catalyst is shown in Figure 3 b. An anisotropic, platelet-like morphology of crystalline α-Fe domains a few nanometers in size is observed at the edge of the large aggregates.

In conclusion, we have provided experimental evidence that validates the understanding obtained on iron model catalysts from surface science experiments conducted at low pressures and theoretical model approaches for the industrial high-pressure ammonia synthesis reaction. No major dynamic phase changes due to nitridation were observed on an industrial ammonia synthesis catalyst when it was subjected to self-generated NH_3 (viz. ND_3) at a concentration of 12.6 vol % at 75 bar and 425 °C, that is, close to the conditions of the Haber–Bosch process. The stability of the α-Fe phase in the catalyst could not be expected based on the thermodynamics of pure iron at such ammonia partial pressures. In comparison to reference Fe, the industrial catalyst shows a complex and defective microstructure that arises in the preparation and activation processes. Also this unique microstructure was stable and hardly any structural healing was observed during 88 h of operation. The absence of nitridation is thus not due to the general absence of a gap between low and high pressure, but can be rather explained by the cancellation of the expected pressure effect by the materials effect. While the former thermodynamically favors bulk nitridation, the latter kinetically stabilizes the defective α-Fe phase—likely a result of the presence of additives and of the Mittasch catalyst synthesis. The complex real structure of this catalyst after activation and its stability appear to be a prerequisite for high performance and should be the target of any alternative synthesis approaches for ammonia synthesis catalysts aiming at a simpler and more elegant preparation.

Experimental Section

The BASF S6-10 catalyst was carefully reduced, dried, transferred through use of an Ar glovebox into the flow cell for the neutron experiment and sealed air-tight. The experiment was carried out on the high-resolution thermal neutron diffractometer SPODI[17] at the research reactor Heinz Maier-Leibnitz (FRM II) of the Technical University Munich in Garching, Germany. For the in situ studies a modified version of a continuous-flow cell was used, which was already described elsewhere.[16a] At the beamline, the prereduced catalyst was activated by heating up slowly from RT to 180 °C with a heating rate of $1\,\mathrm{K\,min^{-1}}$ in a D_2 stream of $9.6\,\mathrm{L\,h^{-1}}$ at 4.4 bar. Further heating to reaction state was done under 75 bar $D_2/N_2/Ar$ syngas (72:23:6) with a rate of $0.5\,\mathrm{K\,min^{-1}}$ to 425 °C. The reaction slowly approached a steady-state concentration of ND_3 of 12.6 vol % after 88 h TOS, which is close to equilibrium. For each reaction state, prereaction, in situ (TOS = 0 and 88 h) and postreaction, three diffraction pattern (each 30 min) were acquired and the ND_3 yield was determined by bubbling the exhaust stream through water and subsequent titration. Analysis of the patterns was carried out by Rietveld refinement and pattern decomposition. Further details of the experiment and the evaluation can be found in the Supporting Information.

Received: July 4, 2013
Published online: October 9, 2013

Keywords: catalyst microstructure · Haber–Bosch process · heterogeneous catalysis · iron nitridation · neutron diffraction

---

[1] F. Haber, R. Le Rossignol, *Z. Elektrochem. Angew. Phys. Chem.* **1913**, *19*, 53.

[2] L. E. Apodaca, U. S. Geological Survey, **2011**.

[3] M. Appl in *Ullmann's Encyclopedia of Industrial Chemistry*, Wiley-VCH, Weinheim, **2000**, pp. 139.

[4] A. Mittasch, *Adv. Catal.* **1950**, *2*, 81.

[5] A. Baranski, A. Kotarba, J. M. Lagan, A. Pattek-Janczyk, E. Pyrczak, A. Reizer, *Appl. Catal. A* **1994**, *112*, 13.

[6] a) G. Ertl, M. Huber, N. Thiele, *Z. Naturforsch. A* **1979**, *34*, 30; b) G. Ertl, *Catal. Rev.* **1980**, *21*, 201; c) G. Ertl, *J. Vac. Sci. Technol. A* **1983**, *1*, 1247; d) F. Bozso, G. Ertl, M. Grunze, M. Weiss, *J. Catal.* **1977**, *49*, 18; e) G. Ertl, N. Thiele, *Appl. Surf. Sci.* **1979**, *3*, 99.

[7] a) M. Boudart, *Catal. Rev. Sci. Eng.* **1981**, *23*, 1; b) M. Boudart, A. Delbouille, J. A. Dumesic, S. Khammouma, H. Topsøe, *J. Catal.* **1975**, *37*, 486.

[8] N. D. Spencer, R. C. Schoonmaker, G. A. Somorjai, *J. Catal.* **1982**, *74*, 129.

[9] H. Topsøe, J. A. Dumesic, M. Boudart, *J. Catal.* **1973**, *28*, 477.

[10] a) K. Honkala, A. Hellman, I. N. Remediakis, A. Logadottir, A. Carlsson, S. Dahl, C. H. Christensen, J. K. Nørskov, *Science* **2005**, *307*, 555; b) P. Stoltze, J. K. Nørskov, *Phys. Rev. Lett.* **1985**, *55*, 2502.

[11] a) E. Lehrer, *Z. Elektrochem.* **1930**, *36*, 460; b) B. Kooi, M. J. Somers, E. J. Mittemeijer, *Metall. Mater. Trans. A* **1996**, *27*, 1063; c) B. Kooi, M. J. Somers, E. Mittemeijer, *Metall. Mater. Trans. A* **1996**, *27*, 1055; d) M. A. J. Somers, B. J. Kooi, L. Maldzinski, E. J. Mittemeijer, A. A. V. D. Horst, A. M. V. D. Kraan, N. M. V. D. Pers, *Acta Mater.* **1997**, *45*, 2013; e) P. Schaaf, *Progr. Mater. Sci.* **2002**, *47*, 1; f) M. Widenmeyer, R. Niewa, T. C. Hansen, H. Kohlmann, *Z. Anorg. Allg. Chem.* **2012**, *638*, 1628.

[12] R. Pelka, I. Moszynska, W. Arabczyk, *Catal. Lett.* **2009**, *128*, 72.

[13] B. Herzog, D. Herein, R. Schlögl, *Appl. Catal. A* **1996**, *141*, 71.

[14] a) J. Block, G. Schulz-Ekloff, *J. Catal.* **1973**, *30*, 327; b) J. A. Dumesic, H. Topsøe, M. Boudart, *J. Catal.* **1975**, *37*, 513.

[15] C. J. H. Jacobsen, S. Dahl, B. S. Clausen, S. Bahn, A. Logadottir, J. K. Nørskov, *J. Am. Chem. Soc.* **2001**, *123*, 8404.

[16] a) T. Kandemir, D. Wallacher, T. Hansen, K.-D. Liss, R. N. d'Alnoncourt, R. Schlögl, M. Behrens, *Nucl. Instrum. Methods Phys. Res. Sect. A* **2012**, *673*, 51; b) T. Kandemir, F. Girgsdies, T. C. Hansen, K.-D. Liss, I. Kasatkin, E. L. Kunkes, G. Wowsnick, N. Jacobsen, R. Schlögl, M. Behrens, *Angew. Chem.* **2013**, *125*, 5271 – 5276; *Angew. Chem. Int. Ed.* **2013**, *52*, 5166 – 5170.

[17] M. Hölzel, A. Senyshyn, N. Juenke, H. Boysen, W. Schmahl, H. Fuess, *Nucl. Instrum. Methods Phys. Res. Sect. A* **2012**, *667*, 32.

[18] W. Mahdi, J. Schütze, G. Weinberg, R. Schoonmaker, R. Schlögl, G. Ertl, *Catal. Lett.* **1991**, *11*, 19.

[19] R. Schlögl, *Ammonia Synthesis*, *Vol. 5*, Wiley-VCH, Weinheim, **2008**.

[20] a) R. Hosemann, A. Preisinger, W. Vogel, *Ber. Bunsenges. Phys. Chem.* **1966**, *70*, 796; b) J. R. Jennings, *Catalytic Ammonia Synthesis—Fundamentals and Practice*, Springer, New York, **1991**.

[21] a) A. Nielsen, *Catal. Rev.* **1981**, *23*, 17; b) W. S. Borghard, M. Boudart, *J. Catal.* **1983**, *80*, 194l; c) G. Weinberg, B. Beran, M. Muhler, R. Schlögl, A. Dent, T. Rayment, *Appl. Catal. A* **1997**, *163*, 83.

[22] T. Kandemir, F. Girgsdies, I. Kasatkin, E. Kunkes, K.-D. Liss, V. K. Peterson, R. Schlögl, M. Behrens, *J. Phys. Conf. Ser.* **2012**, *340*, 012053.

[23] a) M. Leoni, T. Confente, P. Scardi, *Z. Kristallogr. Suppl. 23* **2006**, 249; b) I. Lucks, P. Lamparter, E. J. Mittemeijer, *J. Appl. Crystallogr.* **2004**, *37*, 300; c) R. K. Khatirkar, B. S. Murty, *Mater. Chem. Phys.* **2010**, *123*, 247.

[24] H. Ludwiczek, A. Preisinger, A. Fischer, R. Hosemann, A. Schönfeld, W. Vogel, *J. Catal.* **1978**, *51*, 326.

[25] I. Alstrup, I. Chorkendorff, S. Ullmann, *J. Catal.* **1997**, *168*, 217.

[26] B. Holme, J. Tafto, *Philos. Mag. A* **2000**, *80*, 373.